

October 14, 2015

Tests of Higgs boson compositeness through the HHH form factor.

G.J. Gounaris^a and F.M. Renard^b

^aDepartment of Theoretical Physics, Aristotle University of Thessaloniki,
Gr-54124, Thessaloniki, Greece.

^bLaboratoire Univers et Particules de Montpellier, UMR 5299
Université Montpellier II, Place Eugène Bataillon CC072
F-34095 Montpellier Cedex 5.

Abstract

We show how the q^2 -dependence of the triple Higgs boson HHH form factor can reveal the presence of various types of new physics contributions, like new particles coupled to the Higgs boson or Higgs boson constituents, without directly observing them. We compare the effect of such new contributions to the one of higher order SM corrections to the point-like HHH coupling, due to triangle, 4-leg and s.e. diagrams. We establish simple analytic expressions describing accurately at high energy these SM corrections, as well as the examples of new physics contributions.

PACS numbers: 12.15.-y, 12.60.-i, 14.80.-j

1 Introduction

In spite of the discovery [1] of the Higgs boson [2], as expected in the standard model (SM) [3], the SM cannot be the last word, and physics beyond SM (BSM) should exist [4, 5].

Various types of proposals have been made for this, in particular Higgs boson compositeness [6], leading for example to anomalous Higgs boson couplings [7], or to couplings of the Higgs boson to new visible or invisible particles [8].

There are many processes (involving Higgs boson production or decay) where effective Higgs boson couplings differing from SM predictions could be observed. However in most of them the Higgs boson is on-shell and such a departure could not obviously tell whether it is caused by Higgs compositeness. Also if the Higgs boson is coupled to an invisible sector, this fact will not be directly observable.

We recall that the observation of a suitable Higgs boson form factor could give answers to such questions. Indeed a composite particle (like the proton or the pion) should have a form factor. This means an appropriate q^2 dependence (with some scale) in this form factor. But contrarily to the case of the proton and the pion, we do not have a γHH or a ZHH vertex for studying the H form factor.

In this paper we propose to look at the HHH form factor, that is at a $q^2 \equiv s$ dependence of the HHH vertex when one H , with momentum q , is off-shell. There are various processes which involve the HHH coupling, but not necessarily the form factor with one H far off-shell, like the one we are interested in. Examples of adequate processes or subprocesses are $\mu^+\mu^- \rightarrow H \rightarrow HH$, $ZZ \rightarrow H \rightarrow HH$, $W^+W^- \rightarrow H \rightarrow HH$ and $gg \rightarrow H \rightarrow HH$ (with g denoting the gluon) and $\gamma\gamma \rightarrow H \rightarrow HH$. The first three of these examples are particularly simple; they involve the usual initial tree level H coupling and the final HHH form factor. The last two ones involve a more complex initial 1-loop H coupling.

In SM, in addition to the point-like HHH coupling, the HHH vertex receives order α contributions from the usual scalars, fermions and gauge bosons, due to triangle, bubble with 4-leg couplings and H self-energy diagrams. We compute them in Sec. 2 and we illustrate their corresponding (modest) s dependence. We establish, for each of them, simple analytic expressions valid at high s .

In Sec. 3 we compute examples of new contributions which could be induced either by Higgs boson compositeness or by the couplings of the Higgs boson to a new set of particles. We also give their corresponding simple high s expressions. Illustrations show how such contributions can generate spectacular differences in the s dependence of the HHH form factor, with respect to the one predicted by the SM.

Conclusions and outlooks are given in Sec. 4.

2 SM contributions to the HHH form factor.

The SM prediction for the HHH form factor consists in a zero order contribution given by the point-like coupling

$$eg_{HHH} = -\frac{3em_H^2}{2s_W m_W} \quad , \quad (1)$$

and the higher order corrections. We compute them when one H is off-shell, with its squared four-momentum denoted as $q^2 \equiv s$, while the two other H (with four-momenta p, p') are on-shell.

At first α order, these corrections consist in 1-loop triangles, bubbles with a 4-leg couplings and H self-energy. Up to this order, this form factor is written as

$$F^{SM}(s) = eg_{HHH} + A^{SM}(s) \quad , \quad (2)$$

where in $A^{SM}(s)$ the aforementioned 1-loop SM corrections are collected.

Before discussing them, we mention that these 1-loop diagrams contain divergent terms which should be canceled by appropriate counter terms. There are various possibilities for making these cancelations, which differ by small constant terms. As we are essentially interested only in the high s dependence, we will use the supersimple renormalization scheme (SRS) procedure [9, 10], which leads to the simplest expressions in terms of augmented Sudakov logarithms. Among them, we will only need (see [9, 10] for details):

$$\overline{\ln^2 s_X} \equiv \ln^2 s_X + 4L_{HXX} \quad , \quad s_X \equiv \left(\frac{-s - i\epsilon}{m_X^2} \right) \quad , \quad (3)$$

$$\overline{\ln s_{ij}} \equiv \ln s_{ij} + b_0^{ij}(m_H^2) - 2 \quad , \quad \ln s_{ij} \equiv \ln \frac{-s - i\epsilon}{m_i m_j} \quad , \quad (4)$$

where explicit expressions for $b_0^{ij}(m_H^2)$ and L_{HXX} are given e.g. in Eqs.(A.6, A.5) of [10].

We note that the counter terms needed in the SRS scheme respect this augmented Sudakov structure [9, 10]. Globally this procedure consists in replacing the divergent terms related to the (i, j) internal lines of any contributing diagram, as

$$\ln \frac{-s - i\epsilon}{\mu^2} - \Delta \rightarrow \ln s_{ij} + b_0^{ij}(m_H^2) \quad , \quad (5)$$

where μ denotes the renormalization scale and $\Delta = 1/\epsilon - \gamma_E + \ln(4\pi)$, with the number of dimensions used for regularization written as $n = 4 - 2\epsilon$.

In the present case, with only triangle and bubble diagrams contributing, there is no ambiguity related to the internal lines (i, j) . They can only be H, Z, W and t , so that we can only have $(ij) = (HH), (ZZ), (WW), (tt)$. The SRS results thus obtained, are always denoted as “sim” in the illustrations.

We next describe the exact expressions for the various triangle and bubble diagrams with 4-leg couplings, as well as their high energy SRS (sim) forms.

2.1 Triangles and bubbles with 4-leg couplings

Scalar (SSS) triangles and (SS) bubbles with a 4-leg SSH coupling.

$$\begin{aligned}
A_{SSS}^{SM}(s) &= -\frac{e\alpha}{4\pi} \left\{ g_{HSS}^3 C_0(s, m_H^2, m_H^2, m_S^2, m_S^2, m_S^2) \right. \\
&\quad \left. + g_{HSS} g_{HHSS} [B_0(s, m_S^2, m_S^2) + 2B_0(m_H^2, m_S^2, m_S^2)] \right\} \\
&\rightarrow -\frac{e\alpha}{4\pi} \left\{ g_{HSS}^3 \frac{\overline{\ln^2 s_S}}{s} + g_{HSS} g_{HHSS} (-\overline{\ln s_{SS}}) \right\} .
\end{aligned} \tag{6}$$

This applies to $SSS = HHH, G^0 G^0 G^0, C^Z C^Z C^Z, G^\pm G^\pm G^\pm, C^\pm C^\pm C^\pm$ triangles and to $SS = HH, G^0 G^0, G^\pm G^\pm$ bubbles, where g_{HHH} is given in (1) and¹

$$\begin{aligned}
g_{HHHH} &= -\frac{3m_H^2}{4s_W^2 m_W^2}, \quad g_{HGG} = -\frac{m_H^2}{2s_W m_W}, \quad g_{HHGG} = \frac{1}{2s_W^2 c_W^2}, \\
g_{HC^Z C^Z} &= -\frac{m_W}{2s_W c_W^2}, \quad g_{HC^\pm C^\pm} = -\frac{m_W}{2s_W}.
\end{aligned} \tag{7}$$

Note that for the ghost loop, there is no 4-leg diagram, and that a global fermionic minus sign has been inserted. In all cases, the internal S mass for $H, G^0, C^Z, G^\pm, C^\pm$ is respectively equal to the one of H, Z, Z, W, W .

Fermion triangles (fff)

Due to the strong mass dependence of the Hff coupling, it is adequate to restrict to the $(ttt) + (\overline{ttt})$ case. The result is

$$\begin{aligned}
A_{ttt}^{SM}(s) &= \frac{e\alpha}{4\pi} \frac{3m_t^3}{2s_W^3 m_W^3} \left\{ 2m_t^3 C_0 + 2m_t [3m_H^2 (C_{21} + C_{22}) + 6p.p' C_{23} \right. \\
&\quad \left. + 3n C_{24} + 2q.p C_{11} + 2q.p' C_{12} + 2m_H^2 C_{11} + 2p.p' C_{12} + q.p C_0] \right\} \\
&\rightarrow \frac{e\alpha}{4\pi} \frac{3m_t^3}{2s_W^3 m_W^3} \left\{ 2m_t \left[\frac{-\overline{\ln^2 s_t}}{4} - \overline{\ln s_{tt}} \right] \right\} .
\end{aligned} \tag{8}$$

Vector triangles (VVV) and bubbles (VV) with a 4-leg $HHVV$ coupling.

$$\begin{aligned}
A_{VVV}^{SM}(s) &= \frac{e\alpha}{4\pi} \left\{ g_{HVV}^3 n C_0 + g_{HVV} g_{HHVV} [2B_0(m_H^2, m_V^2, m_V^2) + B_0(s, m_V^2, m_V^2)] \right\} \\
&\rightarrow -\frac{e\alpha}{4\pi} \left\{ g_{HVV}^3 \frac{2\overline{\ln^2 s_V}}{s} + g_{HVV} g_{HHVV} [-\overline{\ln s_{VV}}] \right\} ,
\end{aligned} \tag{9}$$

applied only to $V = Z, W$, since there are no $HZ\gamma$ or $HHZ\gamma$ couplings. Because of this, the V masses in the SRS forms $\overline{\ln^2 s_V}$ and $\overline{\ln s_{VV}}$ can either be m_Z or m_W .

¹ G^\pm, G^0 denote the SM Goldstone fields and C^\pm, C^Z FP ghosts.

(VVS) **triangles**

$$\begin{aligned}
A_{VVS}^{SM}(s) &= \frac{e\alpha}{4\pi} g_{VSH}^2 g_{VVH}^2 \left\{ m_H^2 (C_{21} + C_{22}) + 2p \cdot p' C_{23} + n C_{24} \right. \\
&\quad \left. + (p \cdot p' + 3q \cdot p) C_{11} + (m_H^2 + 3q \cdot p') C_{12} + 2(q^2 + q \cdot p') C_0 \right\} \\
&\rightarrow \frac{e\alpha}{4\pi} g_{VSH}^2 g_{VVH}^2 \left\{ \frac{1}{2} (\overline{\ln^2 s_V} + \overline{\ln s_{VV}}) \right\} ,
\end{aligned} \tag{10}$$

applied to $ZZG^0, W^\pm W^\pm G^\pm$; compare (9).

(VS) **triangles**

$$\begin{aligned}
A_{VS}^{SM}(s) &= \frac{e\alpha}{4\pi} g_{VSH}^2 g_{VVH}^2 \left\{ m_H^2 (C_{21} + C_{22}) + 2p \cdot p' C_{23} + n C_{24} \right. \\
&\quad \left. + (3m_H^2 - p \cdot p') (C_{11} - C_{12}) + 2(m_H^2 - p \cdot p') C_0 \right\} \\
&\rightarrow \frac{e\alpha}{4\pi} g_{VSH}^2 g_{VVH}^2 \left\{ \frac{1}{4} \overline{\ln^2 s_V} + 2 \overline{\ln s_{VV}} \right\} ,
\end{aligned} \tag{11}$$

applied to $ZG^0Z, W^\pm G^\pm W^\pm$.

(SVV) **triangles**

$$\begin{aligned}
A_{SVV}^{SM}(s) &= \frac{e\alpha}{4\pi} g_{VSH}^2 g_{VVH}^2 \left\{ m_H^2 (C_{21} + C_{22}) + 2p \cdot p' C_{23} + n C_{24} \right. \\
&\quad \left. - (m_H^2 + q \cdot p) C_{11} - (p \cdot p' + q \cdot p') C_{12} + q \cdot p C_0 \right\} \\
&\rightarrow \frac{e\alpha}{4\pi} g_{VSH}^2 g_{VVH}^2 \left\{ -\frac{1}{2} (\overline{\ln^2 s_V} + \overline{\ln s_{VV}}) \right\} ,
\end{aligned} \tag{12}$$

applied to $G^0ZZ, G^\pm W^\pm W^\pm$.

(VSS) **triangles**

$$\begin{aligned}
A_{VSS}^{SM}(s) &= \frac{e\alpha}{4\pi} g_{VSH}^2 g_{SSH}^2 \left\{ -m_H^2 (C_{21} + C_{22}) - 2p \cdot p' C_{23} - n C_{24} \right. \\
&\quad \left. - 2(m_H^2 + q \cdot p) C_{11} - 2(p \cdot p' + q \cdot p') C_{12} - 4q \cdot p C_0 \right\} \\
&\rightarrow \frac{e\alpha}{4\pi} g_{VSH}^2 g_{SSH}^2 \left\{ -\frac{1}{2} \overline{\ln^2 s_V} + \overline{\ln s_{VV}} \right\} ,
\end{aligned} \tag{13}$$

applied to $ZG^0G^0, W^\pm G^\pm G^\pm$.

(SVS) triangles

$$\begin{aligned}
A_{SVS}^{SM}(s) &= \frac{e\alpha}{4\pi} g_{VSH}^2 g_{SSH}^2 \left\{ -m_H^2 (C_{21} + C_{22}) - 2p \cdot p' C_{23} - n C_{24} \right. \\
&\quad \left. - (-m_H^2 + q \cdot p + p \cdot p') C_{11} - (m_H^2 - p \cdot p' + q \cdot p') C_{12} + (p \cdot p' + q \cdot p) C_0 \right\} \\
&\rightarrow \frac{e\alpha}{4\pi} g_{VSH}^2 g_{SSH}^2 \{ \overline{\ln^2 s_V} - \overline{\ln s_{VV}} \} ,
\end{aligned} \tag{14}$$

applied to $G^0 Z G^0, G^\pm W^\pm G^\pm$.

(SSV) triangles

$$\begin{aligned}
A_{SSV}^{SM}(s) &= \frac{e\alpha}{4\pi} g_{VSH}^2 g_{SSH}^2 \left\{ -m_H^2 (C_{21} + C_{22}) - 2p \cdot p' C_{23} - n C_{24} \right. \\
&\quad \left. - (m_H^2 - q \cdot p - p \cdot p') C_{11} - (-m_H^2 + p \cdot p' - q \cdot p') C_{12} + (-q \cdot p' + q \cdot p) C_0 \right\} \\
&\rightarrow \frac{e\alpha}{4\pi} g_{VSH}^2 g_{SSH}^2 \left\{ -\frac{1}{2} \overline{\ln^2 s_V} + \overline{\ln s_{VV}} \right\} ,
\end{aligned} \tag{15}$$

applied to $G^0 G^0 Z, G^\pm G^\pm W^\pm$.

In the above contributions the following couplings are needed

$$\begin{aligned}
g_{ZZH} &= \frac{m_Z}{s_w c_w} , \quad g_{ZZHH} = \frac{1}{2s_w^2 c_w^2} , \\
g_{WWH} &= \frac{m_W}{s_w} , \quad g_{WWHH} = \frac{1}{2s_w^2} , \quad g_{ZGH} = g_{WGH} = \frac{1}{2s_w c_w} .
\end{aligned} \tag{16}$$

2.2 H self-energy

This additional contribution is given by

$$A_{se}^{SM}(s) = - \frac{e g_{HHH}}{s - m_H^2} \Sigma_H(s) , \tag{17}$$

where $\Sigma_H(s)$ is computed from the following diagrams:

Bubbles VV leading to

$$\Sigma_H(s) = \frac{X_1^2}{4\pi^2} [B_0] \rightarrow \frac{X_1^2}{4\pi^2} [-\overline{\ln s_{VV}}] , \tag{18}$$

for which we respectively get

$$\begin{aligned} VV = ZZ &\rightarrow X_1^2 = \frac{e^2 M_W^2}{2s_W^2 c_W^4} , \\ VV = W^\pm W^\mp &\rightarrow X_1^2 = \frac{e^2 M_W^2}{s_W^2} . \end{aligned} \quad (19)$$

Bubbles SV leading to

$$\begin{aligned} \Sigma_H(s) &= -\frac{X_1^2}{16\pi^2} [s(B_0 + B_{21} - 2B_1) + nB_{22}] \\ &\rightarrow -\frac{X_1^2}{16\pi^2} [-2s\overline{\ln s_{SV}}] , \end{aligned} \quad (20)$$

for which we respectively get

$$\begin{aligned} SV = G^0 Z &\rightarrow X_1^2 = \frac{e^2}{4s_W^2 c_W^2} , \\ SV = G^\mp W^\pm &\rightarrow X_1^2 = \frac{e^2}{2s_W^2} . \end{aligned} \quad (21)$$

Bubble tt leading to

$$\begin{aligned} \Sigma_H(s) &= -\frac{1}{4\pi^2} [(s(B_1 + B_{21}) + nB_{22} + m_t^2 B_0) X_1^2] \\ &\rightarrow -\frac{X_1^2}{4\pi^2} [\frac{s}{2} \overline{\ln s_{tt}}] , \end{aligned} \quad (22)$$

with

$$X_1^2 = \frac{3e^2}{4s_W^2 M_W^2} [m_t^2] . \quad (23)$$

Bubbles SS leading to

$$\Sigma_H(s) = \frac{X_1^2}{16\pi^2} [B_0] \rightarrow \frac{X_1^2}{16\pi^2} [-\overline{\ln s_{SS}}] , \quad (24)$$

with

$$X_1^2 = \frac{9e^2 m_H^4}{8s_W^2 M_W^2} , \frac{e^2 m_H^4}{8s_W^2 M_W^2} , \frac{e^2 m_H^4}{4s_W^2 M_W^2} , -\frac{e^2 m_W^2}{4s_W^2 c_W^4} , -\frac{e^2 m_W^2}{2s_W^2} , \quad (25)$$

for

$$SS = HH, G^0 G^0, G^+, G^-, C^Z C^Z, C^+ C^- , \quad (26)$$

respectively. Note that in these SS bubbles, the internal S mass is correspondingly equal to the mass of H, Z, W, Z, W .

2.3 Illustrations

Summing the above contributions, either the exact ones or their high energy SRS “sim” forms, we obtain in Figs.1 the SM predictions for A^{SM} as functions of \sqrt{s} .

In the upper row of Fig.1, the left panel corresponds to (ttt) obtained from (8), the middle panel to (HHH) derived from (6), while the right panel refers to $(VVV + GGG + CCC)$ derived from (6, 9).

In the middle row, the left panel corresponds to $(VVS + VSV + SVV)$ obtained from (10,11,12), the middle panel to $(VSS + SVS + SSV)$ obtained from (13, 14, 15), while the right panel shows the Higgs self energy contribution derived from the expressions in Subsection 2.2.

Finally, in the panel at the lowest row, we present the complete F^{SM} result of (2).

As seen from Fig.1, the ttt part (upper left panel) is quickly dominating above the $t\bar{t}$ threshold.

Fig.1 also shows that the shapes of the real and imaginary parts of the various contributions are quite different. This may be useful in case of a departure from the SM prediction is observed². It could for example suggest what type of new contribution should be added.

Note also that the SRS (sim) approximation is globally OK above $\sim 1.5\text{TeV}$.

3 Examples of new physics contributions.

In a pure compositeness picture there is no Born HHH point-like vertex. The whole HHH coupling should then come from an effective (XXX) triangles made by the constituents X and an effective HXX coupling related to the binding.

On another hand, if the Higgs boson is connected to a new sector, one may have triangles involving the corresponding new particles.

In the case of a strong sector (similarly to the hadronic case), there may be resonances R leading to HHH contributions of the type $H \rightarrow R(XX) \rightarrow HH$.

In Figs.2 we have made illustrations of the contributions to the (HHH) form factor corresponding to these examples.

- For a scalar Higgs-constituent X , we get

$$\begin{aligned} A_{XXX}(s) &= -\frac{e\alpha}{4\pi} g_{HXX}^3 C_0(s, m_H^2, m_H^2, m_X^2, m_X^2, m_X^2) \\ &\rightarrow -\frac{e\alpha}{4\pi} g_{HXX}^3 \frac{\ln^2 s_X}{2s} \end{aligned} \quad (27)$$

- for a fermionic constituent F , we get

$$A_{FFF}(s) = -\frac{e\alpha}{4\pi} g_{HFF}^3 \left\{ 2m_F^3 C_0 + 2m_F \left[3m_H^2 (C_{21} + C_{22}) + 6p \cdot p' C_{23} + 3nC_{24} \right] \right\}$$

²See examples in the next Section.

$$\begin{aligned}
& +2q.pC_{11} + 2q.p'C_{12} + 2m_H^2 C_{11} + 2p.p'C_{12} + q.pC_0 \Big] \Big\} \\
& \rightarrow -\frac{e\alpha}{4\pi} g_{HFF}^3 \left\{ 2m_F \left[\frac{-\overline{\ln^2 s_F}}{4} - \overline{\ln s_{FF}} \right] \right\} , \tag{28}
\end{aligned}$$

- and for a typical resonance effect we get

$$A_{Res}(s) = \frac{g_{HR}g_{RHH}}{s - M_R^2 + iM_R\Gamma_R} . \tag{29}$$

Effective couplings have been chosen so that the resulting HHH form factor is similar to the SM one. In such a case, the illustrations serve to emphasize the different s -dependencies. In Figs.2a,b,c one indeed sees that the s dependencies appearing in these examples are very different from each other and also very different from the SM case.

So we believe that there is much to be learned from the measurement of the HHH form factor.

4 Conclusions and outlooks.

We have computed the real and imaginary parts of the SM 1-loop contributions to the HHH form factors, as well as examples of possible new physics effects corresponding either to Higgs boson compositeness or to the coupling of the Higgs boson to a new sector.

We have emphasized the fact that the $q^2 \equiv s$ dependencies of the HHH form factor can be very different, depending on their origin. As it can be seen in the illustrations these differences can be spectacular and reflect the specific nature of the new physics (bosonic or fermionic constituents or resonances).

In each case we have also given the corresponding analytic expressions in the adequate “sim” approximation, allowing a quick estimate of the effect at high s .

The aim of this paper was only to put forward this idea of looking especially at the s -dependence of the form factors and to show that such effects may exist.

We hope that these results will encourage further phenomenological and experimental studies of the possibilities to measure the HHH form factor.

In the simplest situation, this form factor appears in the process $\mu^- \mu^+ \rightarrow HH$, (about the $\mu^- \mu^+$ collider project see [11]). It appears through the s-channel H exchange diagram, which is proportional to the $H\mu\mu$ coupling. There exist also t and u channel μ^\pm exchange diagrams, but their contribution is suppressed, since it is quadratic in the $H\mu\mu$ coupling. Complete 1-loop corrections to these Born terms are then needed, in order to be able to compare the effects of new HHH contributions, to the exact SM prediction, see [12].

The subprocesses $ZZ \rightarrow HH$ and $W^+W^- \rightarrow HH$ also involve the simple s-channel H exchange diagram associated with a 4-leg $ZZHH$ or W^+W^-HH vertex. In addition, t and u channel Z or W exchanges contribute. These subprocesses can be reached at e^-e^+ colliders or at LHC, by making a detailed analysis.

The processes $gg \rightarrow HH$ and $\gamma\gamma \rightarrow HH$ contain an s-channel H exchange, but the initial vertex needs a 1-loop contribution. There are also other 1-loop diagrams producing the final HH state. Specific works should be devoted to each of these processes, see e.g. [13, 14, 15, 16].

References

- [1] G. Aad *et al.* (ATLAS Collaboration), Phys. Lett. **B716**, 1 (2012). S. Chatrchyan *et al.* (CMS Collaboration), Phys. Lett. **B716**, 30 (2012), arXiv:1207.7235 [hep-ex]. Gavin J. Davies (CDF and D0 Collaborations), Front. Phys. China **8**, 270 (2013). ATLAS Collaboration: <https://twiki.cern.ch/twiki/bin/view/AtlasPublic/HiggsPublicResults>. CMS Collaboration: <https://twiki.cern.ch/twiki/bin/view/CMSPublic/PhysicsResultsHIG>.
- [2] P. Higgs, Phys. Lett. **12**, 132 (1964); Phys. Rev. Lett. **13**, 508 (1964); Phys. Rev. **145**, 1156 (1966)); F. Englert and R. Brout, Phys. Rev. Lett. **13**, 321 (1964); G. Guralnik, C. Hagen and T. Kibble, Phys. Rev. Lett. **13**, 585 (1964).
- [3] John Ellis, [arXiv:1312.5672]. S. Dawson *et al* (Higgs working group) [arXiv:1310.8361], M. Klute, R. Lafaye, T. Plehn, M. Rauch and D. Zerwas, Eur. Phys. J. **101**, 51001 (2013). A. Djouadi, Phys. Rept. **459**, 1 (2008). J. Gunion, H. Haber, G. Kane and S. Dawson, *The Higgs Hunter's Guide* (Addison-Wesley, Reading, MA, 1990). S. Heinemeyer, Int. J. Mod. Phys. **A21**, 2659 (2006).
- [4] E. Massó, JHEP **10**, 2014 (128). E. Massó and V. Sanz, Phys. Rev. **D87**, 033001 (2013). H. Bélusca-Maïto, arXiv:1507.05657. For an introduction on the connections between the muon $g - 2$ and dark matter, see e.g. G. Bélanger, C. Delaunay and S. Westhoff, arXiv:1507.06660.
- [5] M.E. Peskin, arXiv:1506.08185; M. Muhlleitner, arXiv:1410.5093; Ben Gripaios, arXiv:1503.02636, arXiv:1506.05039; E. Massó, arXiv:1406.6376; H. Bélusca-Maïto, arXiv:1507.05657.
- [6] G. Panico and A. Wulzer, arxiv: 1506.01961 [hep-ph].
- [7] S.Kumar, P.Poulose and S.Sahoo, Rev. **D91**, 073016(2015).
- [8] B.Patt and F. Wilczek, hep-ph/0605188.
- [9] G.J. Gounaris and F.M. Renard, Acta Phys. Polon. **42**, 2107 (2011); Phys. Rev. **D86**, 013003 (2012); Phys. Rev. **D90**, 073007 (2014).
- [10] G.J. Gounaris and F.M. Renard, Phys. Rev. **D88**, 113003 (2013).
- [11] Y. Alexahin et al, FERMILAB-CONF-13-245T, arXiv: 1308.2143.

- [12] G.J. Gounaris and F.M. Renard, in preparation.
- [13] S.Dawson, A.Ismail and I.Low, Phys. Rev. **D91**, 115008 (2015).
- [14] V.I. Telnov, JINST 9(2014)09, arXiv:1409.5563.
- [15] E. Asakawa *et al*, Phys. Rev. **D82**, 115002 (2010).
- [16] A. Levy, CLICdp-Conf-2015-001, arXiv:1501.02614.

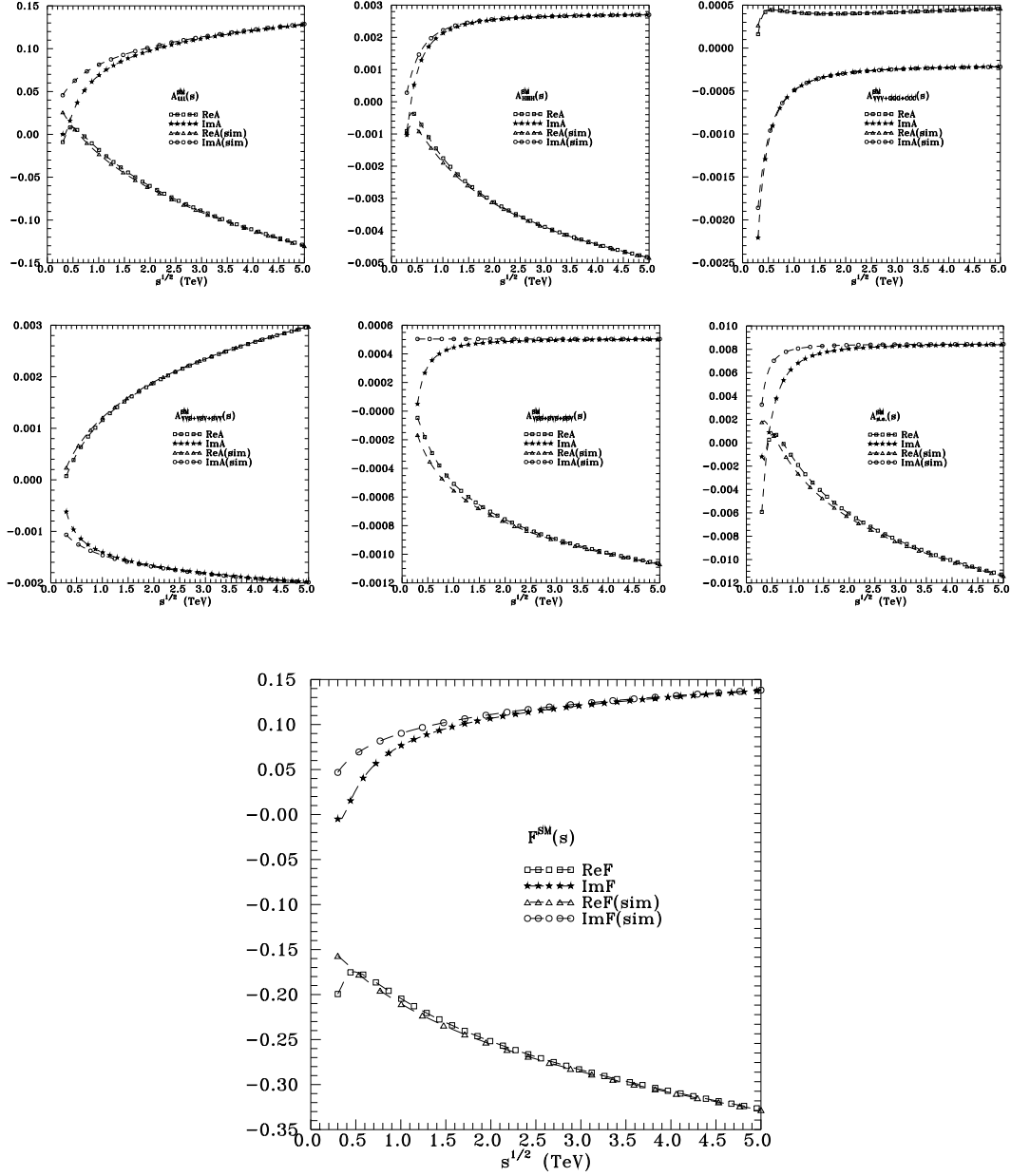


Figure 1: The upper two rows describe the real and imaginary parts of the various SM contributions to the A^{SM} form factors in (2), in the exact 1-loop treatment and in its high energy SRS (“sim”) approximation; see text in Section 2.3. The panel in the third row gives the corresponding total SM contribution F^{SM} defined in (2).

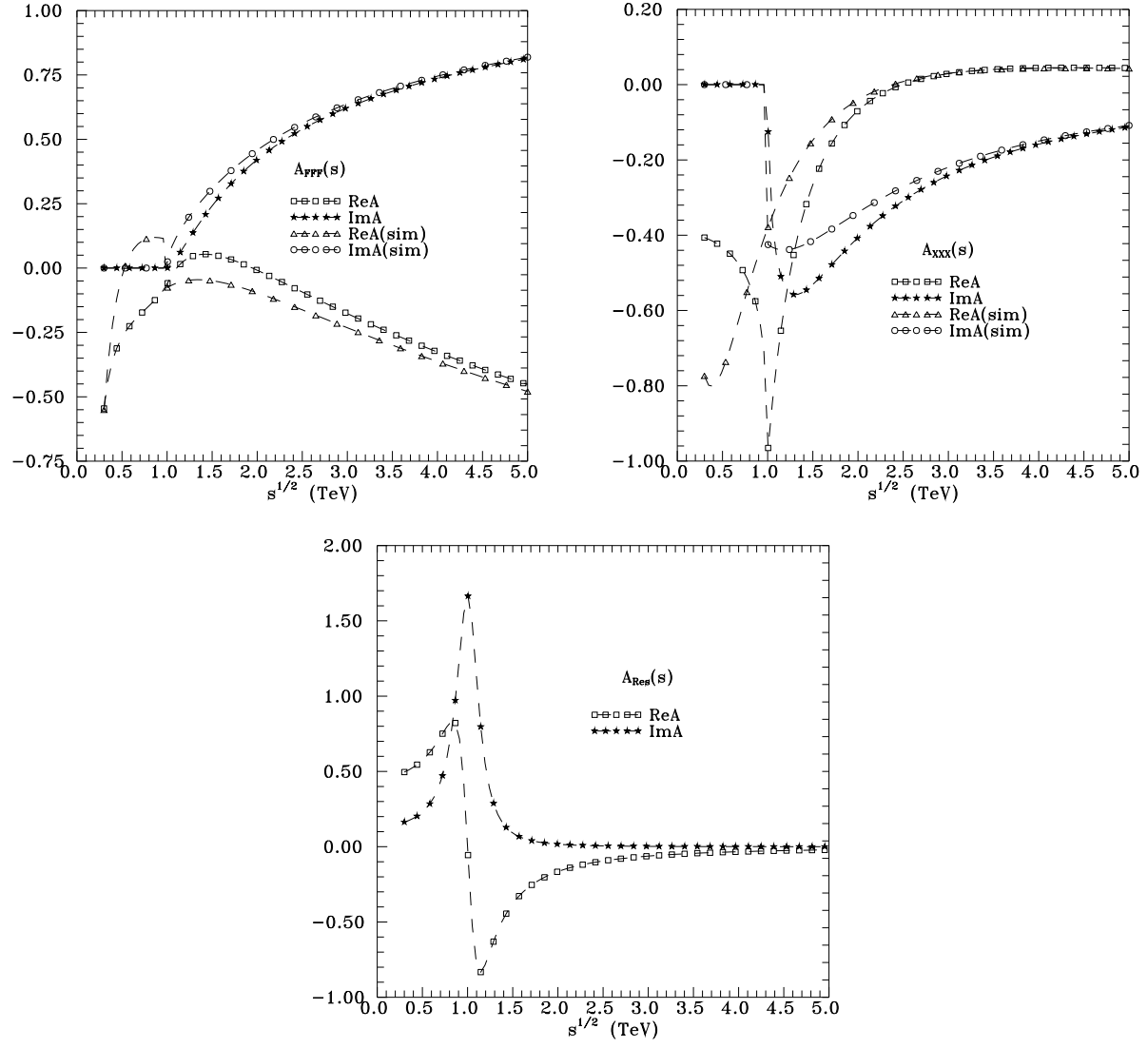


Figure 2: New physics contributions to the HHH form factors. Upper left panel gives the example of $A(s)_{FFF}$ of (28), upper right gives the example of $A(s)_{XXX}$ of (27), while the lower panel the example of $A(s)_{\text{Res}}$ of (29).